NJC

Detection of phosphates in water utilizing a Eu3+-mediated relay mechanism

Journal:	*New Journal of Chemistry*
Manuscript ID	NJ-ART-09-2021-004578.R1
Article Type:	Paper
Date Submitted by the Author:	15-Dec-2021
Complete List of Authors:	Farshbaf, Sepideh; Bowling Green State University DEY, KAUSTAV; Bowling Green State University, Chemistry Mochida, Wakana; Tokyo Metropolitan University - Minamiosawa Campus Kanakubo, Masashi; Tokyo Metropolitan University - Minamiosawa Campus Nishiyabu, Ryuhei; Tokyo Metropolitan University - Minamiosawa Campus Kubo, Yuji; Tokyo Metropolitan University, Division of Applied Chemistry, Faculty of Urban Environmental Sciences Anzenbacher, Pavel; Bowling Green State University, Chemistry

ARTICLE

Detection of phosphates in water utilizing a Eu³⁺-mediated relay mechanism

Sepideh Farshbaf,[a] Kaustav Dey, [a] Wakana Mochida,[b] Masashi Kanakubo,[b] Ryuhei Nishiyabu,[b] Yuji Kubo,*[b] and Pavel Anzenbacher, Jr.*[a]

Three carboxamidequinoline ligands were synthesized and their complexes with Eu³⁺ were used for recognition and detection of organic/inorganic phosphates in water. The signal transduction process is based on an "On-Off-On" switch in the fluorescence signal utilizing changes in the intramolecular charge transfer (ICT). The fluorescence emission of ligands is quenched upon exposure to the Eu³⁺ (Off signal). Following the addition of the phosphate analytes the ligand-Eu³⁺ complex disassembles, which results in the regeneration of the original emission of the ligand (On signal). In general, the Eu³⁺ complexes show higher affinity towards adenosine 5'-triphosphate (ATP) and lower affinity to other phosphates, namely adenosine 5'-diphosphate (ADP), adenosine 5'-monophosphate (AMP), pyrophosphate ($H_2P_2O_7^{2-}$, PPi), and dihydrogenphosphate ($H_2PO_4^-$, Pi).

Introduction

Organic and inorganic phosphates are important in a range of chemical and biological processes. For example, among various organic phosphates, adenosine 5'-triphosphate (ATP) known as the cell's energy currency provides the energy for metabolisms within cells.[1] It also participates in DNA duplication,[2] cellular respiration,[3] signaling transduction[4,5] and enzymatic reactions.[6,7] Cellular ATP concentration is about 1-10 mmol/L, and ca. 1 µmol/L in human plasma.[8] Any anomaly in the ATP level can be used as a diagnostic marker of diseases such as Alzheimer's disease,[9–11] glaucoma,[12–14] and lower urinary symptom (LUTS).[15,16] Likewise, inorganic phosphates play central roles in the environment and biology. Most of the naturally occurring phosphates are not toxic with the exception of organophosphorus pesticides that have been found to show a range of toxicity after chronic exposure.[17] Additionally, while phosphate fertilizers are beneficial for agriculture, over-supply of phosphate results in the pollution of natural water sources due to eutrophication, algal bloom, and aquatic dead-zones.[18] Phosphate is also a crucial component in the body. Kidneys are responsible for balancing the concentration of phosphate in the blood, which is between 0.8–1.45 mM in healthy individuals.[19] Any failure in kidney function can lead to phosphate related disorders such as hyperphosphatemia, which is a major factor

of morbidity and mortality in hemodialysis patients.[20] Due to the importance of organic phosphates such as nucleotide phosphates as well as inorganic phosphates, recognition, detection, and quantitative determination of this important class of analytes is essential for biochemical studies and clinical diagnoses. A number of techniques such as HPLC,[21] bioluminescence methods,[22] electrochemical methods,[23] immunoassays,[24] and others have been developed for analysis of phosphates. These, however, frequently require advanced instrumentation and trained personnel. Thus, optical methods such as fluorescence methods are becoming increasingly popular.[25]

Among the luminescence-based sensors for phosphate anions, the lanthanide complexes of fluorescent ligands became increasingly popular in the past few decades and a number of studies on the topic was published[26–34] and recently reviewed.[35–40] In most cases, however, these studies utilize the lanthanide-centered emission for signal transduction. Interestingly, a concept of metal extrusion to achieve Off-On signal in the presence of phosphate anions has also been investigated.[41–47] These systems frequently utilize the paramagnetic Cu²⁺ or Fe³⁺ metal ions, which offer the advantage of switching luminescence to achieve efficient signal transduction for anion detection and are thus interesting platforms for sensing of phosphates.

Here, we decided to investigate carboxyamidoquinoline-based compounds **1**-**3** (Scheme 1 and 2) and study their utility in phosphate sensing. Easy synthesis, bright fluorescence, and a ligand cleft capable of binding metal ions including Eu³⁺ make these ligands suitable for sensing anions such as phosphates utilizing an On-Off-On mechanism.

a. Department of Chemistry and Center for Photochemical Sciences, Bowling Green State University, Bowling Green, OH, 43403 (USA), E-mail: pavel@bgsu.edu
b. Department of Applied Chemistry, Graduate School of Urban Environmental Sciences, Tokyo Metropolitan University, Tokyo 192-0397 (Japan), E-mail: yujik@tmu.ac.jp.
c. Electronic Supplementary Information (ESI) available: Fluorescence and UV-Vis spectra, and Job-plot experiments. See DOI: 10.1039/x0xx00000x

Results and discussion

Synthesis of the ligands 1-3

Three carboxamidequinoline-based ligands **1**-**3** were synthesized according to the Schemes 1 and 2, and characterized by ^{1}H and ^{13}C NMR, mass spectrometry, and elemental analysis. Briefly, N-Boc protected glycine was reacted with ethyl chloroformate to yield the corresponding mixed anhydride, which upon treatment with 8-aminoquinoline **4** gave the N-Boc protected 2-amino-N-(quinolin-8-yl)acetamide **5**. Compound **5** was treated with trifluoroacetic acid to remove the Boc protection to yield 2-amino-N-(quinolin-8-yl)acetamide **6**, which was then subjected to condensation with salicylaldehyde followed by an addition of sodium borohydride to achieve a reductive amination to obtain ligand **1**. Similarly (Scheme 2), 2-hydroxy-5-methylbenzaldehyde **7** was reacted with 2-aminobenzene thiol to obtain 2-(benzo[*d*]thiazol-2-yl)-4-methylphenol **8**, which was subjected to Duff formylation (with hexamethylene tetramine) to obtain 3-(benzo[d]thiazol-2-yl)-2-hydroxy-5-methylbenzaldehyde **9**. Condensation of compound **9** and 2-amino-N-(quinolin-8-yl)acetamide gave ligand **2**. The reductive amination of ligand **2** gave ligand **3**.
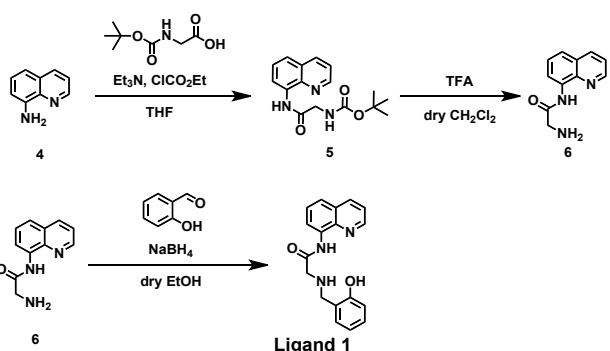
Scheme 1: Synthesis of **1**
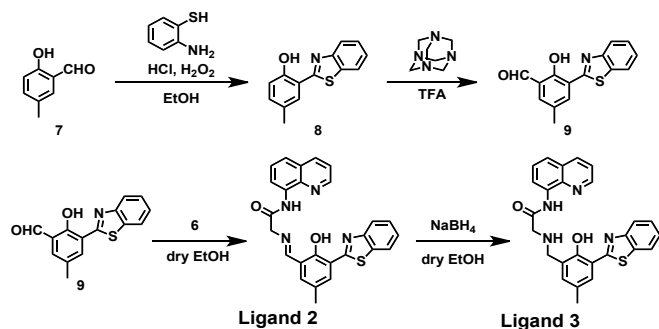
Scheme 2: Synthesis of **2** and **3**

On-Off-On signalling based on a relay mechanism

To achieve strong signal transduction, we used a fluorescence-based relay recognition approach.[48] The fluorescence quantum yields of the ligands are: **1** Φ_{FL} 1.2%, **2** Φ_{FL} 12.1%, **3** Φ_{FL} 3.8%, and correlate with the presence of the secondary amine moiety, which quenches the ligand emission due to the photo-induced electron transfer (PET). Conversely, the imine (Ligand 2) which does not support PET shows significantly higher fluorescence quantum yield. Here, we utilized the ability of ligands **1-3** to bind metal cations including Eu^{3+}.[49] This process is accompanied by quenching of the original ligand fluorescence (Off signal) (Fig. 1) as one would have expected from the paramagnetic ions.[41,50] However, the Eu^{3+} centered luminescence owing to the energy transfer from ligands to the lanthanide known as the antenna effect was not observed.[51,52] This is presumably due to the presence of water, which is known to quench the Eu^{3+} emission.[53] In addition to the water-mediated quenching mentioned above, the lack of Eu^{3+} emission could also be due to the competition with other relaxation pathways such as phosphorescence of the ligand, and back energy transfer resulting from the energy gap less than ca. 1800 cm^{-1} between the triplet state of the ligand and the emissive state of the europium.[54,55] In the presence of phosphate anions, the phosphates form very stable Eu-anion complexes (characterized by the solubility product $K_{SP} < 10^{-25}$).[56] Thus, the Eu^{3+} quencher is removed from the Eu^{3+}-ligand complex and the original ligand fluorescence is restored providing a clearly observable turn-On signal (Fig. 1).
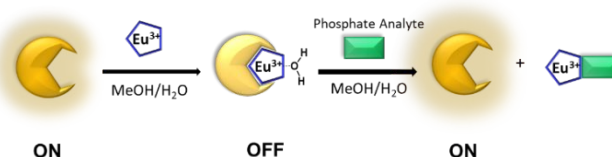

Figure 1: Graphic illustration of the relay recognition technique.

Studies of ligand-metal assembly

The amidoquinoline moiety and the hydroxy group of the ligands' phenol enable the Eu^{3+} coordination by the ligands. The formation of the complexes of the ligands **1**-**3** with Eu^{3+} was studied using UV-vis and fluorescence spectroscopy. The spectral changes and the resulting isotherms clearly showed the saturation of the changes upon addition of one equivalent of Eu^{3+}. In the case of ligands **1** and **2**, the fitting data as well as Job's plots indicate 1:1 stoichiometry of the complexes (Figures S33-S34). In the case of **3**, however, the spectral behaviour suggests a formation of 2:1 complex (**3**:Eu^{3+}) followed by a formation 1:1 complex at higher Eu^{3+} concentration. This is also supported by the Job's plot (Figure S35). The titrations with anions were then performed at **3**:Eu^{3+} concentrations corresponding to the 1:1 [**3**-Eu].

Here, the amidoquinoline moiety in **1** shows the absorption band at 313 nm and the corresponding emission at 405 nm (Fig. 2). Upon binding Eu^{3+} to the ligand **1**, a hypsochromic shift was observed in both the absorption and emission. This can be attributed to the lower efficiency of the intramolecular charge transfer (ICT) from the donor (N of amide) to the acceptor (quinoline). Binding the Eu^{3+} to the nitrogen of the amide group (donor) decreases the electron donating character of the

nitrogen and leads to the delocalization of ground and excited states. This results in the observed blue shift in both absorption and fluorescence spectra (Fig. 2).[57,58]
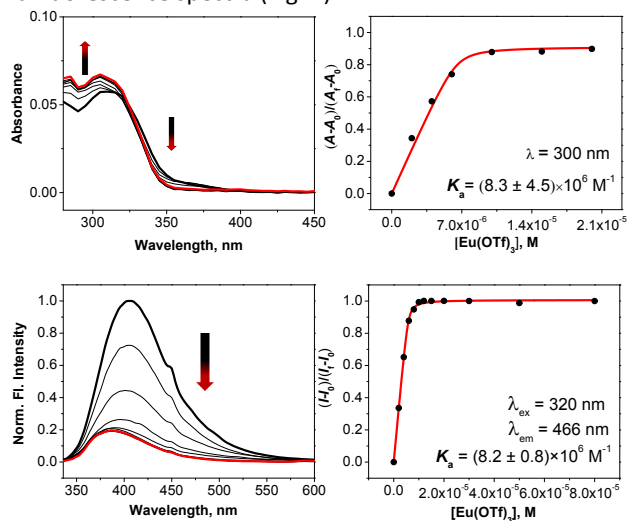

Figure 2: Absorption (top) and fluorescence (bottom) titration spectra and the corresponding isotherms of **1** (10.0 μM) upon the addition of incremental amounts of Eu(OTf)$_3$ in wet MeOH (~2% water).

In the spectra of **2** and **3**, in addition to the amidoquinoline absorption band at 313 nm, additional bands at 360 nm and 340 nm were observed, respectively (Fig. 3 and 4, top). These bands originate from the 2-(2-benzothiazolyl) phenol moiety.

Coordination of the Eu^{3+} to **2** and **3** quenches the emission of the ligand. This change is associated with decreased ICT efficiency upon the binding of Eu^{3+} to the carboxyamido-quinoline moiety. Also, the emission of the 2-(benzo[*d*]thiazol-2-yl)-4-methylphenol moiety was quenched only to the residual emission maximum at 550 nm in **2** (Fig. 3, bottom). As stated above, the ligand **3** complexation showed a biphasic behavior as a result of formation of 2:1 complex (**3**:Eu^{3+}) followed by a formation 1:1 (Fig. 4, bottom).
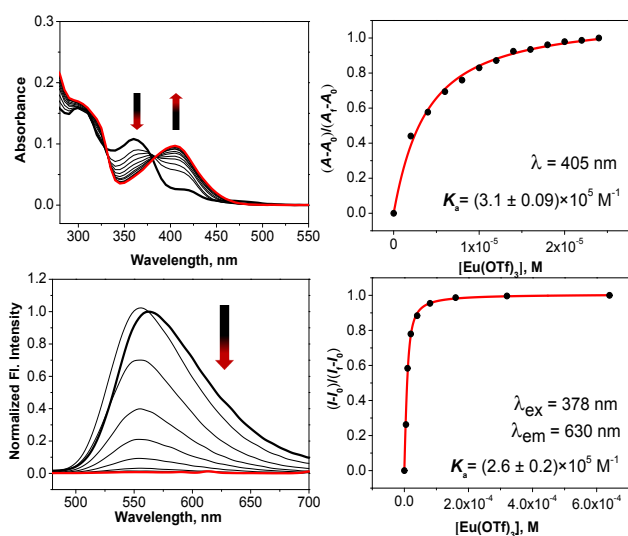

Figure 3: Absorption (top) and fluorescence (bottom) titration spectra and the corresponding isotherms of **2** (10.0 μM) upon the addition of incremental amounts of Eu(OTf)$_3$ in wet MeOH (~2% water).
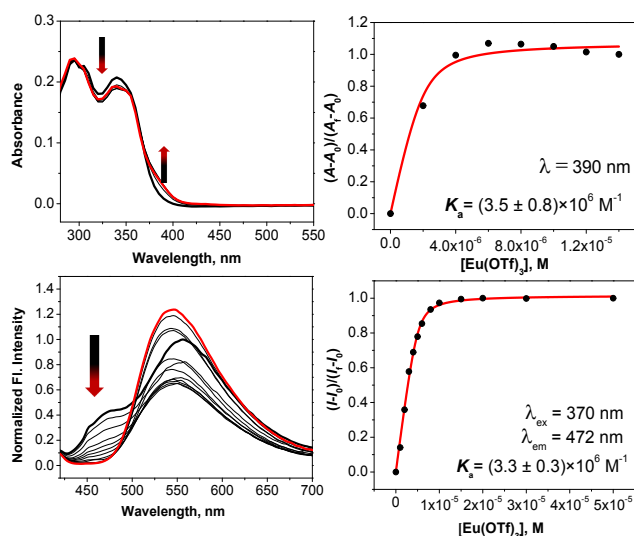

Figure 4: Absorption (top) and fluorescence (bottom) titration spectra and the corresponding isotherms of **3** (10.0 μM) upon the addition of incremental amounts of Eu(OTf)$_3$ in wet MeOH (~2% water).

The association constants for the formation of the [**1**-Eu]–[**3**-Eu] complexes determined from the fluorescence titration are 8.2×10^6 M^{-1}, 2.6×10^5 M^{-1} and 3.3×10^6 M^{-1}, respectively.

"Off-On" type fluorescence responses of the ensembles to anions

The phosphate analyte sensing was studied in UV-Vis and fluorescence titration experiments. The behavior of the ligands was investigated in the presence of Eu^{3+} upon the addition of the sodium salts of biologically active phosphates (ATP, ADP, AMP), and inorganic phosphates (pyrophosphate, dihydrogenphosphate) in water. The complexes of [**1**-Eu]–[**3**-Eu] undergo disassembly upon the incremental addition of anions due to interaction of the analyte with Eu^{3+}. This is, in general, accompanied by the regeneration of the absorption and emission of the spectra of the free ligand. The ligands exhibit different behavior in the presence of different anions due to the structure of the ligand and analyte.

As shown in Figures 2-4 and the binding constants there, the ligand **1** forms the most stable Eu^{3+} complex from the three ligands **1**-**3**. This is also reflected by the magnitudes for the apparent binding constants for the removal of the Eu^{3+} from the complexes. As expected, **1** then shows the lowest apparent affinity constants for the phosphate analytes. This may be explained by the lack of the steric hindrance in **1** associated with the presence of the benzo[*d*]thiazole moiety in the close vicinity of the Eu^{3+} binding site.

In general, the incremental addition of the phosphates, namely ATP, ADP, AMP, PPi, and Pi to [**1**-Eu] results in the amplification of the emission intensity of the ligand (Fig. 5). However, the amount of the analyte required to regenerate the original emission fluorescence intensity of the ligand is related to the

structure of the phosphate analyte. For example, a stoichiometric amount of ATP is required to remove the europium and regenerate the ICT fluorescence of the free **1**, while higher concentrations of ADP, PPi, and Pi are required to remove the europium from the [**1**-Eu].

These observations are reflected by the order of apparent affinity constants of ATP >> PPi > ADP > Pi > AMP (Table 1). The apparent affinity constant of [**1**-Eu] and ATP is 1.0×10^6 M^{-1}, which is 18 times more than the apparent affinity constant recorded for ADP (5.5×10^4 M^{-1}). The role of the adenine nucleobase is not as significant as the number of the phosphate moieties. Thus, the PPi gives only a slightly better response than ADP for all three ligands. For example, [**1**-Eu] shows $K_{PPi} = 7.9 \times 10^4$ M^{-1} while $K_{ADP} = 5.5 \times 10^4$ M^{-1}, and [**2**-Eu] yields the corresponding apparent affinity constants, $K_{PPi} = 2.0 \times 10^6$ M^{-1} while $K_{ADP} = 1.3 \times 10^6$ M^{-1}. Similar effects are observed for Pi and AMP. Taken together, this suggests that the adenine presents a small but not negligible steric hindrance for the approach of the corresponding phosphate to the ligand-Eu^{3+} complex. The preliminary experiments with GTP suggest that the nature of the nucleobase does not play a significant difference in the ligand selectivity.[59]

Interestingly, the analyte addition of greater than 2 equivalents of ADP, AMP, phosphate, and pyrophosphate, respectively, to [**3**-Eu] results in what appears to be deprotonation of the phenolic group. This is followed by the decrease in the intensity

Table 1. Apparent affinity constants were obtained by fluorescence titrations.

	Apparent affinity constants, M^{-1}		
Anions[a]	[**1**-Eu]	[**2**-Eu]	[**3**-Eu]
ATP	$(1.0 \pm 0.3) \times 10^6$	$(4.2 \pm 0.8) \times 10^6$	$(6.1 \pm 1.4) \times 10^6$
ADP	$(5.5 \pm 0.4) \times 10^4$	$(1.3 \pm 0.2) \times 10^6$	$(4.0 \pm 0.8) \times 10^6$
AMP	ND[b]	$(6.9 \pm 1.5) \times 10^5$	$< 10^5$ [b]
Pi	$(1.1 \pm 0.02) \times 10^4$	$(1.1 \pm 0.1) \times 10^6$	$(3.3 \pm 0.3) \times 10^6$
PPi	$(7.9 \pm 0.4) \times 10^4$	$(2.0 \pm 0.5) \times 10^6$	$(7.6 \pm 1.6) \times 10^6$

[a] All anions were in the form of sodium salts in water. All the titrations were repeated at least three times. [b] Constant could not be determined due to multiple equilibria that appear to be involved.

of the emission at ca. 550 nm of the free ligand accompanied by the amplification in the emission (470 nm) (Scheme 3). The positions of the maxima and the changes in the relative intensity follow the process observed during the titration with diluted hydroxide. Scheme 3 represents this proposed mechanism. Upon the addition of analyte and disassembly of the complex, the emission of the complex (black) was amplified (blue) (Scheme 3, left). Following the addition of more than 2 equivalents of the analyte, **3** undergoes deprotonation of the phenol group which results in the decrease of the emission intensity (blue to red) due to the formation of the deprotonated form of the ligand (scheme 3, right).
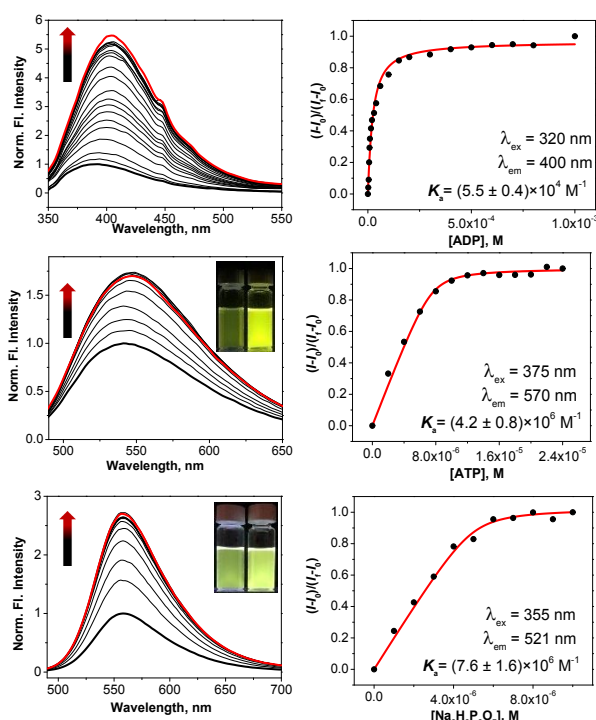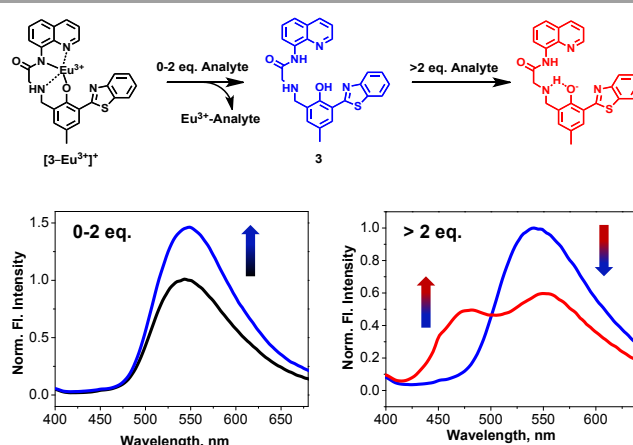

Scheme 3: (Top) Schematic representation of the proposed mechanism of addition of 2 equivalents and more than 2 equivalents of an analyte to **3**. (Bottom) Fluorescence spectra of addition of 1 equivalent and more than 1 equivalent of analyte.

Figure 5: (Top) Fluorescence titration spectra and isotherm of [**1**-Eu] ([**1**] = 10.0 μM, [Eu(OTf)$_3$] = 10.0 μM) upon the addition of ADP. (Center) Fluorescence titration spectra and isotherm of [**2**-Eu] ([**2**] = 10.0 μM, [Eu(OTf)$_3$] = 10.0 μM) upon the addition of ATP. Photograph of 10.0 μM [**2**-Eu] complex (left vial) vs [**2**-Eu] after addition of 30 μM ATP (right vial). (Bottom) Fluorescence titration spectra and isotherm of [**3**-Eu] ([**3**] = 10.0 μM, [Eu(OTf)$_3$] = 10.0 μM) upon the addition of Na$_2$H$_2$P$_2$O$_7$. Photograph of 10.0 μM [**3**-Eu] complex (left vial) vs [**3**-Eu] after addition of 30 μM Na$_2$H$_2$P$_2$O$_7$ (right vial).

Conclusions

In summary, three carboxyamidoquinolines (**1-3**) have been studied for recognition of organic and inorganic anions, namely ATP, ADP, AMP, pyrophosphate, and phosphate in water. Self-assembly of the ligands with an equivalent amount of Eu^{3+} suppresses the emissive ICT state, which quenches the fluorescence of **1-3** providing an On-Off signal. In the presence of phosphate analytes, the ligand-Eu^{3+} complexes disassemble, i. e. the Eu^{3+} quencher is removed from the complex, a process that results in the regeneration of the fluorescence emission of

the ligands and a clearly observable Off-On signal. In general, [**1**-Eu] shows lower affinities for the phosphates, followed by [**2**-Eu] and [**3**-Eu] with the highest affinities for the phosphates. This reflects the affinities for Eu^{3+} complexes. The order of the apparent affinities for [**1**-Eu] is ATP >> PPi > ADP > Pi ≈ AMP, for [**2**-Eu] is ATP > PPi > ADP > Pi > AMP, and for [**3**-Eu] is PPi ≈ ATP > Pi ≈ ADP > AMP. Thus, the highest relative selectivity for ATP was observed for [**1**-Eu]. The highest affinity for ATP is rationalized by the three phosphate moieties involved in the complexation to Eu^{3+}, followed by the anions with two phosphate moieties (PPi and ADP), and finally by anions with one phosphate (Pi and AMP). Our results show the **1-3** carboxyamidoquinolines to form complexes with Eu^{3+} and that the resulting ensembles can be successfully leveraged in sensing of phosphates with Off-On fluorescence signaling.

Conflicts of interest

There are no conflicts to declare.

Notes and references

1 J. R. Knowles, *Annu. Rev. Biochem.*, 1980, **49**, 877–919.

2 X. Shen, G. Mizuguchi, A. Hamiche and C. Wu, *Nature*, 2000, **406**, 541–544.

3 K.-Y. Tan, C.-Y. Li, Y.-F. Li, J. Fei, B. Yang, Y.-J. Fu and F. Li, *Anal. Chem.*, 2017, **89**, 1749–1756.

4 A. V. Gourine, E. Llaudet, N. Dale and K. M. Spyer, *Nature*, 2005, **436**, 108–111.

5 P. B. Dennis, A. Jaeschke, M. Saitoh, B. Fowler, S. C. Kozma and G. Thomas, *Science*, 2001, **294**, 1102–1105.

6 Y. Xu, J. Xu, Y. Xiang, R. Yuan and Y. Chai, *Biosens. Bioelectron.*, 2014, **51**, 293–296.

7 E. H. Abraham, P. Okunieff, S. Scala, P. Vos, M. J. S. Oosterveld, A. Y. Chen, B. Shrivastav and G. Guidotti, *Science*, 1997, **275**, 1324–1326.

8 M. W. Gorman, E. O. Feigl and C. W. Buffington, *Clin. Chem.*, 2007, **53**, 318–325.

9 C. Zhang, R. A. Rissman and J. Feng, *J. Alzheimers Dis.*, 2015, **44**, 375–378.

10 S. Przedborski and M. Vila, *Clin. Neurosci. Res.*, 2001, **1**, 407–418.

11 G. Burnstock, *Trends Pharmacol. Sci.*, 2006, **27**, 166–176.

12 C. H. Mitchell, W. Lu, H. Hu, X. Zhang, D. Reigada and M. Zhang, *Purinergic Signalling*, 2009, **5**, 241–249.

13 A. Li, X. Zhang, D. Zheng, J. Ge, A. M. Laties and C. H. Mitchell, *Exp. Eye Res.*, 2011, **93**, 528–533.

14 B. M. Davis, L. Crawley, M. Pahlitzsch, F. Javaid and M. F. Cordeiro, *Acta Neuropathol.*, 2016, **132**, 807–826.

15 S. P. Kelley, H. R. Courtneidge, R. E. Birch, A. Contreras-Sanz, M. C. Kelly, J. Durodie, C. M. Peppiatt-Wildman, C. K. Farmer, M. P. Delaney, J. Malone-Lee, M. A. Harber and S. S. Wildman, *SpringerPlus*, 2014, **3**, 200.

16 K. Gill, H. Horsley, A. S. Kupelian, G. Baio, M. De Iorio, S. Sathiananamoorthy, R. Khasriya, J. L. Rohn, S. S. Wildman and J. Malone-Lee, *BMC Urol.*, 2015, **15**, 7.

17 S. Chen and J. R. Cashman, in *Advances in Molecular Toxicology*, eds. J. C. Fishbein and J. M. Heilman, Elsevier, 2013, vol. 7, pp. 207–233.

18 D. Cordell, J.-O. Drangert and S. White, *Glob. Environ. Change*, 2009, **19**, 292–305.

19 E. Slatopolsky, A. M. Robson, I. Elkan and N. S. Bricker, *J. Clin. Invest.*, 1968, **47**, 1865–1874.

20 J.-P. Gutzwiller, D. Schneditz, A. R. Huber, C. Schindler, F. Gutzwiller and C. E. Zehnder, *Nephrol., Dial., Transplant.*, 2002, **17**, 1037–1044.

21 P. Yeung, L. Ding and W. L. Casley, *J. Pharm. Biomed. Anal.*, 2008, **47**, 377–382.

22 A. R. Ribeiro, R. M. Santos, L. M. Rosário and M. H. Gil, *J. Bioulumin. Chemilumin.*, 1998, **13**, 371–378.

23 S. Berchmans, T. B. Issa and P. Singh, *Anal. Chim. Acta*, 2012, **729**, 7–20.

24 C. Chen, J. Zhao, Y. Lu, J. Sun and X. Yang, *Anal. Chem.*, 2018, **90**, 3505–3511.

25 S. Pal, T. K. Ghosh, R. Ghosh, S. Mondal and P. Ghosh, *Coord. Chem. Rev.*, 2020, **405**, 213128.

26 J. Sahoo, R. Arunachalam, P. S. Subramanian, E. Suresh, A. Valkonen, K. Rissanen and M. Albrecht, *Angew. Chem., Int. Ed.*, 2016, **55**, 9625–9629.

27 S. H. Hewitt, G. Macey, R. Mailhot, M. R. J. Elsegood, F. Duarte, A. M. Kenwright and S. J. Butler, *Chem. Sci.*, 2020, **11**, 3619–3628.

28 M. R. Ganjali, M. Hosseini, Z. Memari, F. Faridbod, P. Norouzi, H. Goldooz and A. Badiei, *Anal. Chim. Acta*, 2011, **708**, 107–110.

29 Zainelabdeen. H. Mohamed, T. Soukka, C. Arenz and M. Schäferling, *ChemistrySelect*, 2018, **3**, 12430–12439.

30 X. Liu, J. Xu, Y. Lv, W. Wu, W. Liu and Y. Tang, *Dalton Trans.*, 2013, **42**, 9840–9846.

31 J. Massue, S. J. Quinn and T. Gunnlaugsson, *J. Am. Chem. Soc.*, 2008, **130**, 6900–6901.

32 C. M. G. dos Santos and T. Gunnlaugsson, *Dalton Trans.*, 2009, 4712.

33 J. I. Bruce, R. S. Dickins, L. J. Govenlock, T. Gunnlaugsson, S. Lopinski, M. P. Lowe, D. Parker, R. D. Peacock, J. J. B. Perry, S. Aime and M. Botta, *J. Am. Chem. Soc.*, 2000, **122**, 9674–9684.

34 S. J. A. Pope, B. P. Burton-Pye, R. Berridge, T. Khan, P. J. Skabara and S. Faulkner, *Dalton Trans.*, 2006, 2907.

35 S. E. Bodman and S. J. Butler, *Chem. Sci.*, 2021, **12**, 2716–2734.

36 J. Wongkongkatep, A. Ojida and I. Hamachi, *Top. Curr. Chem.*, 2017, **375**, 30.

37 A. B. Aletti, D. M. Gillen and T. Gunnlaugsson, *Coord. Chem. Rev.*, 2018, **354**, 98–120.

38 S. Shinoda and H. Tsukube, *Analyst*, 2011, **136**, 431–435.

39 D. Parker, J. D. Fradgley and K.-L. Wong, *Chem. Soc. Rev.*, 2021, **50**, 8193–8213.

40 M. L. Aulsebrook, B. Graham, M. R. Grace and K. L. Tuck, *Coord. Chem. Rev.*, 2018, **375**, 191–220.

41 M. V. R. Raju, S. M. Harris and V. C. Pierre, *Chem. Soc. Rev.*, 2020, **49**, 1090–1108.

42 Q. Meng, Y. Wang, M. Yang, R. Zhang, R. Wang and Z. Zhang, *RSC Adv.*, 2015, **5**, 53189–53197.

43 J. Wu, Y. Gao, J. Lu, J. Hu and Y. Ju, *Sens. Actuators, B*, 2015, **206**, 516–523.

ARTICLE

44 Z. Chen, L. Wang, G. Zou, X. Cao, Y. Wu and P. Hu, *Spectrochim. Acta, Part A*, 2013, **114**, 323–329.

45 P. Saluja, N. Kaur, N. Singh and D. O. Jang, *Tetrahedron Letters*, 2012, **53**, 3292–3295.

46 J. Hatai, S. Pal and S. Bandyopadhyay, *Tetrahedron Lett.*, 2012, **53**, 4357–4360.

47 H. Goh, Y. G. Ko, T. K. Nam, A. Singh, N. Singh and D. O. Jang, *Tetrahedron Lett.*, 2016, **57**, 4435–4439.

48 S. Suganya, S. Naha and S. Velmathi, *ChemistrySelect*, 2018, **3**, 7231–7268.

49 M. Pushina, S. Farshbaf, W. Mochida, M. Kanakubo, R. Nishiyabu, Y. Kubo and P. Anzenbacher, Jr., *Chem. - Eur. J.*, 2021, 202100896R1.

50 A. Ramdass, V. Sathish, E. Babu, M. Velayudham, P. Thanasekaran and S. Rajagopal, *Coord. Chem. Rev.*, 2017, **343**, 278–307.

51 S. I. Weissman, *J. Chem. Phys.*, 1942, **10**, 214–217.

52 K. Binnemans, *Coord. Chem. Rev.*, 2015, **295**, 1–45.

53 J.-C. G. Bünzli, *Coord. Chem. Rev.*, 2015, **293–294**, 19–47.

54 A. de Bettencourt-Dias, P. S. Barber and S. Viswanathan, *Coord. Chem. Rev.*, 2014, **273–274**, 165–200.

55 S. Shuvaev, M. Starck and D. Parker, *Chem. - Eur. J.*, 2017, **23**, 9974–9989.

56 F. H. Firsching and S. N. Brune, *J. Chem. Eng. Data*, 1991, **36**, 93–95.

57 B. Valeur and I. Leray, *phosphate analysis*, 2000, **205**, 3–40.

58 K. Boonkitpatarakul, A. Smata, K. Kongnukool, S. Srisurichan, K. Chainok and M. Sukwattanasinitt, *J. Lumin.*, 2018, **198**, 59–67.

59 V. E. Zwicker, G. E. Sergeant, E. J. New and K. A. Jolliffe, *Org. Biomol. Chem.*, 2021, **19**, 1017–1021.